Optical rectification in a traveling-wave geometry

U. Peschel,* K. Bubke, D. C. Hutchings, J. S. Aitchison, and J. M. Arnold

Department of Electronics and Electrical Engineering, University of Glasgow, Glasgow G12 8QQ, United Kingdom
(Received 22 June 1999)

We study the generation of microwave pulses due to optical rectification in a traveling-wave geometry. A system of evolution equations is derived which describes the mutual propagation of both optical and microwave fields. Overlap integrals and optimization criteria are given, and analytical expressions to determine the generated microwave pulse are derived. It is observed that in non-velocity-matched geometries two microwave pulses are generated initially. Both are the exact image of the optical signal. One pulse stays attached to the optical wave, while the other propagates at the microwave group velocity and is subject to absorption and dispersive broadening. In contrast, in velocity-matched configurations a single signal is generated which is proportional to the first derivative of the optical pulse. It is found that for increased conversion efficiencies the action of the generated voltage on the optical wave via the electro-optic effect can no longer be neglected, and results in an effective cubic nonlinearity acting on the optical wave. [S1050-2947(99)04011-1]

PACS number(s): 42.65.Ky, 42.79.Nv, 07.57.Hm

I. INTRODUCTION

Second-order nonlinear effects were among the first to be investigated after the invention of the laser. It was shown that frequency doubling occurs if a highly intense beam is incident on a noncentrosymmetric crystal [1]. In early theoretical papers it was pointed out that in addition to a second-harmonic wave a static electrical field should be generated [2]. In fact only a few years later it was demonstrated that a short voltage pulse is induced by an optical pulse propagating through a quartz crystal [3]. Optical rectification has attracted constantly growing interest (for an overview, see e.g. Ref. [4], and references therein). This is because it provides an easy and elegant way to transfer the optical power into an electrical signal, which is available for further processing. In the usual nonresonant case, second-order nonlinearities have an instantaneous response, and therefore the induced electrical signal can in principle be as short as the initial optical pulse. The generated short voltage shock can be used for device testing and sampling applications. Using a pulsed laser operating in the subpicosecond domain, the generated electrical pulse covers a wide frequency range extending to the THz domain [5,6], where efficient sources of coherent radiation are not available to date. Another very promising application of optical rectification is the construction of fast photodiodes, which in principle have no intrinsic delay imposed by the material response. Although much progress has been made toward achieving these goals, the conversion efficiency obtained is rather low and a practical implementation remains to be devised. A breakthrough could be achieved by employing waveguiding structures where the optical and electrical fields propagate in parallel until a certain depletion of the pump pulse is reached. In addition to an increased efficiency, this would be a step toward a further integration and a more practical device scheme. In fact travelling wave electro-optic modulators, where electrical and optical pulses propagate in parallel, come close to this aim.

Unfortunately the theory describing the mutual propagation of an optical and a microwave field coupled together by the second-order nonlinear response of the medium is currently incomplete. The aim of this paper is to develop an appropriate set of evolution equations for the fields propagating in the waveguide structure. We define overlap integrals, which determine the efficiency of the process and provide a tool to optimize the device. Finally we derive analytical expressions to describe the overall conversion process.

In addition to general considerations of traveling-wave optical rectification, the derivation of a consistent description of a system including optical and microwave fields is a challenging task by itself. For example the slowly varying envelope approximation cannot be applied to the microwave domain in a straightforward way, although it has been successfully used to describe the propagation of optical pulses with even less than picosecond duration. Some attempts have been made to describe the propagation of microwave pulses on nonlinear transmission lines, and the resulting evolution equations are usually related to the Boussinesq or to the Korteweg–de Vries equation [7,8]. Here our description of the microwave field comes close to the latter type of equation, while the propagation equation of the optical pulse is much more similar to common equations in optics, which are based on the slowly varying envelope approximation.

II. BASIC EQUATIONS

To illustrate our procedure and to give an impression of the magnitude of the physical quantities involved we investigate a structure (see Fig. 1) already studied in Ref. [9]. It is grown on a heavily doped substrate to provide for the bottom electrode. A GaAs core is sandwiched between two AlAs layers to allow for optical guiding. Lateral confinement is provided by a rib etched into the cladding layer. It is covered with a metal contact which forms the top electrode. The microwave field spreads between both electrodes. To avoid losses due to free-carrier absorption, the structure should be designed in such a way that the optical mode does not extend

*Permanent address: IFTO/PATF, FSU-Jena, Jena, Germany.
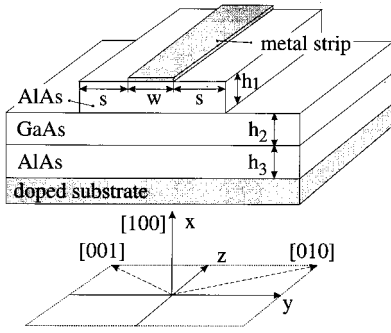
FIG. 1. Structure under investigation (top: geometry; bottom: coordinate system and crystal axes; $s=w=1.8\,\mu$m; $h_1=h_3=0.72\,\mu$m; $h_2=1.065\,\mu$m; GaAs: $\varepsilon_R(\omega=0)=12.9$; $\varepsilon_R(\omega=\omega_{opt})=11.404$; AlAs: $\varepsilon_R(\omega=0)=9.7$, $\varepsilon_R(\omega=\omega_{opt})=8.374$).

to the electrodes. On the other hand, the separation between the two electrodes has to be small to provide a maximum overlap between optical and microwave fields. Because of the usual growth [100] and cleaving [110] directions we assume the vertical direction (x) to be parallel to [100] crystal orientation. The field propagates into the z direction, which corresponds to the [011] direction. Taking into account that in a fcc lattice the only independent nonzero second-order susceptibility tensor element is $d_{14}=\frac{1}{2}\chi^{(2)}_{1,2,3}(\omega,-\omega)=-(1/2)n^4 r_{41}$, the optical field is assumed to be TE polarized (the main component is in the y direction), where the main component of the microwave field should be directed into the x direction (quasi-TM mode). Note that no special care was taken to optimize this structure with respect to maximum overlap integrals nor to obtain group-velocity matching. The values obtained below for this structure are therefore far away from being optimal.

In what follows we start from basic electrodynamics. In the frequency-domain, Maxwell's equations in the absence of free charges or currents read as

$$\nabla\times\mathbf{E}=i\omega\mu_0\mathbf{H},$$

$$\nabla\times\mathbf{H}=-i\omega(\varepsilon_0\varepsilon_R\mathbf{E}+\mathbf{P}^{NL}),\qquad(1)$$

where $\mathbf{E}$ and $\mathbf{H}$ denote the electric and magnetic fields, respectively. Both depend on the angular frequency ω and both are influenced by the nonlinearly induced polarization $\mathbf{P}^{NL}$. The waveguide structure including the metal layers is determined by the relative dielectric constant $\varepsilon_R(x,y)$. ε_0 and μ_0 account for the free-space permittivity and for the free-space permeability, respectively.

Because optical nonlinearities are usually very weak, we first consider the unperturbed case ($\mathbf{P}^{NL}=\mathbf{0}$). Unless otherwise stated, we do not restrict considerations to particular frequency domains, and therefore include both the optical and microwave modes in a consistent description. The waveguide is a single mode with respect to the above-mentioned polarization directions in both the optical and microwave domains. The corresponding unperturbed mode profiles are assumed to be known and to have spatial structures like

$$\mathbf{E}^{unpert}(x,y,z,\omega)=\mathbf{E}^0(x,y,\omega)\exp[i\beta(\omega)z],$$

$$\mathbf{H}^{unpert}(x,y,z,\omega)=\mathbf{H}^0(x,y,\omega)\exp[i\beta(\omega)z]\qquad(2a)$$

where the propagation constant $\beta(\omega)$ is mainly real but might have a small imaginary part in the case of weak losses. The absolute value of the field structures defined in Eq. (2) is chosen in such way that the guided mode power p_0.

$$p_0=2\,\mathrm{Re}\left\{\int dx\int dy[\mathbf{E}^0\times(\mathbf{H}^0)^*]_z\right\},\qquad(2b)$$

does not depend on frequency, and the index z denotes the z component of the Poynting vector. Now we mix perturbed and unperturbed fields and derive the following expression from Eq. (1):

$$\nabla\cdot[\mathbf{E}\times(\mathbf{H}^{unpert})^*+(\mathbf{E}^{unpert})^*\times\mathbf{H}]=i\omega(\mathbf{E}^{unpert})^*\cdot\mathbf{P}^{NL}.\qquad(3)$$

After replacing the unperturbed fields in Eq. (3) by inserting Eq. (2a) into Eq. (3), we integrate over the waveguide structure (x and y directions). Finally only the z component of the vectors on the left-hand side of Eq. (3), remains and we obtain

$$\left[\frac{\partial}{\partial z}-i\beta\right]\int dx\int dy[\mathbf{E}\times(\mathbf{H}^0)^*+(\mathbf{E}^0)^*\times\mathbf{H}]_z$$

$$=i\omega\int dx\int dy(\mathbf{E}^0)^*\cdot\mathbf{P}^{NL},\qquad(4)$$

where only the fields $\mathbf{E}$, $\mathbf{H}$, and $\mathbf{P}^{NL}$ still depend on the propagation direction z.

Because all acting nonlinearities are weak, we can assume that the mode profiles are not changed by the action of the polarization, and that only the amplitudes evolve. Therefore, we decompose the perturbed fields into a constant (but still frequency-dependent) field shape and into an evolving amplitude as

$$\mathbf{E}(x,y,z,\omega)=u(z,\omega)\mathbf{E}^0(x,y,\omega),$$

$$\mathbf{H}(x,y,z,\omega)=u(z,\omega)\mathbf{H}^0(x,y,\omega),\qquad(5)$$

and transform Eq. (4) into

$$\left[\frac{\partial}{\partial z}-i\beta(\omega)\right]u,(z,\omega)$$

$$=\frac{i\omega}{p_0}\int dx\int dy[\mathbf{E}^0(x,y,\omega)]^*\cdot\mathbf{P}^{NL}(x,y,z,\omega).$$

$$(6)$$

Expression (6) describes any field evolution in the frequency domain without making critical assumptions. Unfortunately the nonlinear polarization expressed by the electrical fields gives rise to convolution integrals in the frequency domain, making a deeper insight into the field dynamics virtually impossible. Therefore, the alternative time domain description of Eq. (6) will be derived. To this end we concentrate on the two relevant frequency regimes, i.e., around the carrier frequency of the optical wave ω_{opt} and around the origin $\omega=0$. We now expand the propagation constant $\beta(\omega)$ of the

guided modes around the respective frequencies. In the case of the optical field this expansion is trivial, and results in the following Taylor series:

$$\beta(\omega) = \beta_{opt} + \frac{\omega - \omega_{opt}}{\nu_{opt}} + \frac{D_{opt}}{2}(\omega - \omega_{opt})^2 + \cdots, \quad (7a)$$

where ω_{opt} is the carrier frequency, and β_{opt}, ν_{opt}, and D_{opt} denote the mean propagation constant, the group velocity, and the dispersion of the optical pulse, respectively, defined as,

$$\beta_{opt} = \beta(\omega_{opt}), \quad \frac{1}{\nu_{opt}} = \frac{n_{opt}^{group}}{c} = \frac{\partial \beta}{\partial \omega}\bigg|_{\omega = \omega_{opt}}$$

and

$$D_{opt} = \frac{\partial^2 \beta}{\partial \omega^2}\bigg|_{\omega = \omega_{opt}},$$

where n_{opt}^{group} represents the group index of the optical wave, and c the velocity of light in vacuum.

Because the microwave field is centered around $\omega = 0$, we expand the propagation constant at this point. The reality condition requires $\beta(-\omega) = -\beta(\omega)^*$, and results in the expansion

$$\beta(\omega) = \frac{i}{2}\alpha_{mic} + \frac{\omega}{\nu_{mic}} + \frac{i}{2}\alpha_{mic}''\omega^2 + \frac{T_{mic}}{6}\omega^3 + \cdots, \quad (7b)$$

with

$$\alpha_{mic} = 2\,\text{Im}[\beta(0)], \quad \frac{1}{\nu_{mic}} = \frac{n_{mic}^{group}}{c} = \text{Re}\left(\frac{\partial \beta}{\partial \omega}\bigg|_{\omega=0}\right),$$

$$\alpha_{mic}'' = \text{Im}\left(\frac{\partial^2 \beta}{\partial \omega^2}\bigg|_{\omega=0}\right) \quad \text{and} \quad T_{mic} = \text{Re}\left(\frac{\partial^3 \beta}{\partial \omega^3}\bigg|_{\omega=0}\right)$$

where n_{mic}^{group} is the group index of the microwave mode, which coincides with its effective index at $\omega = 0$, α_{mic} and α_{mic}'' are the linear and nonlinear loss coefficients, respectively and T_{mic} is the dispersion coefficient. Note that in Eq. (7b) purely real and purely imaginary coefficients alternate. The expansion around zero frequency is always justified unless the microwave spectrum touches material resonances, especially those of lattice vibrations. In this case the latter frequency domain has to be treated separately, and a further evolution equation for the evolving phonon mode has to be taken into account. Here we restrict our considerations to the simplest case, where no additional resonances influence the field evolution. For both the microwave and optical fields we terminated our expansion after the first dispersive term, which causes the pulse to spread even in the absence of losses. In general the field profiles which enter the overlap integrals in Eq. (5) also exhibit some frequency dependence. However, a considerable part of this has been removed by the normalization to the frequency-independent guided mode power p_0 introduced in Eq. (2b). In what follows it is assumed that the field structures are invariant within each separate optical and microwave regime (but normally differ be-

tween the two regimes). Some remarks on the influence of their frequency dependence on the final evolution equations will be made later.

A further difficulty may arise if one tries to evaluate the field structures defined in Eq. (2a), the guided power (2b), or the propagation constants (7b) exactly at zero frequency. Strictly speaking, all these quantities are defined as results of a limiting procedure toward static conditions. It turns out that for vanishing frequencies all fields are transversal ($E_z = 0$) and real valued. In this case it is convenient to replace the optical power by an electrical one p_{el}:

$$p_{el} = \frac{p_0}{2} = \lim_{\omega \to 0} \text{Re}\left\{\int dx \int dy [\mathbf{E}^0 \times (\mathbf{H}^0)^*]_z\right\} = \frac{U^2}{Z},$$

which can be expressed in terms of the voltage U between both electrodes and by the impedance Z of the structure. Also, most of the other quantities which define the microwave propagation can be expressed by common electrostatic quantities, as was done in Ref. [8].

Now we insert Eq. (7) into Eq. (6) and perform the inverse Fourier transform. We end up with propagation equations in the time domain for the microwave and optical fields, respectively:

$$\left[\frac{\partial}{\partial z} + \frac{\alpha_{mic}}{2} + \frac{1}{\nu_{mic}}\frac{\partial}{\partial t} - \frac{\alpha_{mic}''}{2}\frac{\partial^2}{\partial t^2} - \frac{T_{mic}}{6}\frac{\partial^3}{\partial t^3}\right]u_{mic}(z,t)$$

$$= -\frac{1}{2p_{el}}\frac{\partial}{\partial t}\int dx \int dy \mathbf{E}_{mic}^0(x,y,\omega=0)\cdot\mathbf{P}_{mic}(x,y,z,t),$$

$$(8a)$$

$$\left[\frac{\partial}{\partial z} + \frac{1}{\nu_{opt}}\frac{\partial}{\partial t} + i\frac{D_{opt}}{2}\frac{\partial^2}{\partial t^2}\right]u_{opt}(z,t)$$

$$= \frac{1}{p_0}\left(i\omega_{opt} - \frac{\partial}{\partial t}\right)$$

$$\times \int dx \int dy [\mathbf{E}_{opt}^0(x,y,\omega_{opt})]^* \cdot \mathbf{P}_{opt}(x,y,z,t),$$

$$(8b)$$

The fast varying phases (i.e., $\exp[i\beta(\omega_{opt})z - i\omega_{opt}t])$ have been removed from Eq. (8b). The total electrical field is now constructed as

$$\mathbf{E}(x,y,z,t) = \lfloor u_{opt}(z,t)\mathbf{E}_{opt}^0(x,y)\exp(i\beta_{opt}z - i\omega_{opt}t) + c.c.\rfloor$$

$$+ u_{mic}(z,t)\mathbf{E}_{mic}^0(x,y),$$

where c.c. denotes the complex conjugate. The nonlinearly induced polarization is decomposed into different frequency components as

$$\mathbf{P}^{NL}(x,y,z,t) = [\mathbf{P}_{opt}(x,y,z,t)\exp(i\beta_{opt}z - i\omega_{opt}t) + c.c.]$$

$$+ \mathbf{P}_{mic}(x,y,z,t).$$

Although the optical field is described in a complex notation, in the nonresonant case the nonlinear polarization is in phase with the driving field, and all quantities related to the microwave fields are real. Note that the driving term of the micro-

wave evolution is the first time derivative instead of the non-linearly induced polarization itself. In contrast the optical field is influenced directly. Now we are going to express the relevant components of the nonlinear polarization by the electrical field explicitly, while taking into account only the main polarization directions. Hence we assume that the optical field is polarized in the y (TE) direction, and the microwave field in the x (TM) direction and end up with the expressions:

$$[\mathbf{P}_{\text{mic}}]_x = -\frac{\varepsilon_0}{2}\chi^{(2)}\ [\mathbf{E}_{\text{opt}}^0]_y^2|u_{\text{opt}}|^2$$

and

$$[\mathbf{P}_{\text{opt}}]_y = -\varepsilon_0\chi^{(2)}[\mathbf{E}_{\text{mic}}^0]_x[\mathbf{E}_{\text{opt}}^0]_y u_{\text{mic}} u_{\text{opt}}, \qquad (9)$$

where $\chi^{(2)}$ is the second-order susceptibility of the material. Here it is assumed that the crystal orientation corresponds to the usual configuration depicted in Fig. 1, and the only independent nonzero tensor element is $\chi^{(2)} = \chi_{123}^{(2)}$. For other orientations of the guide or for other material systems the relevant coefficients may vary, but the basic structure of the equations remains the same. Additional terms including a term which solely contains the square of the microwave field may arise if the basic field structures have other polarization components of considerable magnitude. For simplicity, we concentrate on the simplest case sketched above.

Before inserting Eq. (9) into Eq. (8), we normalize all field amplitudes with respect to the respective guided powers,

$$U_{\text{opt}} = \sqrt{p_0}u_{\text{opt}}, \qquad U_{\text{mic}} = \sqrt{p_{\text{el}}}u_{\text{mic}},$$

and end up with the final set of equations as

$$\left[\frac{\partial}{\partial z} + \frac{\alpha_{\text{mic}}}{2} + \frac{1}{\nu_{\text{mic}}}\frac{\partial}{\partial t} - \frac{\alpha''_{\text{mic}}}{2}\frac{\partial^2}{\partial t^2} - \frac{T_{\text{mic}}}{6}\frac{\partial^3}{\partial t^3}\right]U_{\text{mic}}$$

$$= \chi_{\text{eff}}\frac{\partial}{\partial t}|U_{\text{opt}}|^2, \qquad (10a)$$

$$\left[\frac{\partial}{\partial z} + \frac{1}{\nu_{\text{opt}}}\frac{\partial}{\partial t} + i\frac{D_{\text{opt}}}{2}\frac{\partial^2}{\partial t^2} + 2i\omega_{\text{opt}}\chi_{\text{eff}}U_{\text{mic}}\right]U_{\text{opt}}$$

$$= 2\chi_{\text{eff}}\frac{\partial}{\partial t}[U_{\text{mic}}U_{\text{opt}}], \qquad (10b)$$

where the efficiency of the nonlinear coupling between both fields is defined by the following overlap integral:

$$\chi_{\text{eff}} = \frac{\varepsilon_0}{2p_0\sqrt{p_{el}}}\int dx\int dy\chi^{(2)}[\mathbf{E}_{\text{opt}}^0]_y^2[\mathbf{E}_{\text{mic}}^0]_x. \quad (11)$$

Note that both the field structures as well as the nonlinear coefficient $\chi^{(2)}$ depend on x and y. To evaluate all relevant coefficients of the sample depicted in Fig. 1, we determined the microwave mode by solving Laplace's equation in the stationary limit [10]. The optical mode was calculated by a finite-difference scheme similar to that introduced in Ref. [11]. For the tabulated value of the second-order susceptibility for GaAs, $\chi_{123}^{(2)} = 200$ pm/V [12], the overlap integral amounts to $\chi_{\text{eff}} = 8.3 \times 10^{-14}$ s/m$\sqrt{W}$.

It is sometimes more convenient to refer to the generated voltage instead of the power levels. The voltage of the mi-
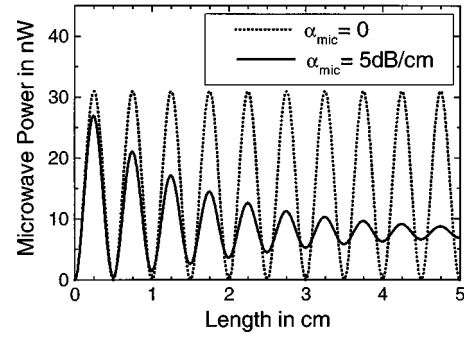
FIG. 2. Microwave generation by two interacting optical waves, power evolution vs distance for finite and vanishing losses (parameters as in Table I).

crowave is defined by the field amplitude as $V_{\text{mic}}(z,t) = \sqrt{Z}U_{\text{mic}}(z,t)$, where Z is the impedance of the structure.

Although the set of equations (10) looks rather complicated it is much easier to be handled than the original Maxwell's equations. Due to the lack of a second derivative in the z direction it separates forward and backward propagation, and both analytical and numerical treatments are simplified considerably. It is interesting to note that the linear part of the above equation for the microwave was previously derived by Jäger to describe the pulse propagation on a nonlinear transmission line [8]. Therefore, intrinsic nonlinearities due to e.g., a carrier motion in the surrounding layers can be easily included without changing the basic structure of the equations. Also, additional terms which arise in the case of mixed polarized microwave fields will not change the essential structure of the equations. Additionally, the optical wave might be influenced by the cubic nonlinearity of the material. Here we neglect those effects, and concentrate on the optical rectification process only. The system of equations (10) accounts for forward-propagating fields only. In fact a backward-propagating microwave could also have been excited. Its evolution equation coincides with that of the forward-propagating field [see Eq. (10a)], except for the opposite sign in front of the z derivative and the nonlinearity. Although the backward field is driven by the same nonlinear term, its amplitude is usually negligible, as we will demonstrate later.

Note that the electro-optic coefficient which describes the action of the dc field on the optical wave is related to the rectification coefficient which drives the microwave field through permutation symmetry [13]. Provided that we are far from material resonances, the electro-optic coefficient ($\omega_{\text{opt}}\chi_{\text{eff}}$) in Eq. (10b) is real and does not give rise to an energy exchange. Energy conservation is ensured by the time derivatives of the remaining nonlinear terms. If we included frequency-dependent field profiles in Eq. (11), additional higher time derivatives of the nonlinear terms would appear.

III. UNDEPLETED PUMP APPROXIMATION

First the case where the amount of generated microwave energy is negligible and the optical wave is almost unaffected by the rectification process will be examined. Further, the dispersive effects on the optical wave shall be neglected ($D_{\text{opt}} = 0$), and the optical wave is assumed to propagate

without any changes. Under these circumstances we have to deal with Eq. (10a) only, and the optical pulse enters as a given inhomogenity of a linear differential equation only. In what follows we also neglect the backreflection at the output of the guide.

A. Two optical frequencies

Strictly speaking, the system of evolution equations (10) defines the microwave field except for an integration con-

stant, which corresponds to a constant dc voltage, and which has to be determined from the boundary conditions. A real power transfer does not occur in the cw case. The most simple nonstationary case is that of an optical field consisting of two frequencies ($\omega_0 \pm \delta\omega$) of equal amplitude which are slightly detuned from each other, and hence generate a beat signal at $\delta\omega$. The optical amplitude is launched as $U_{\text{opt}}(z=0,t)=U_0 \cos(\delta\omega t)$, and the generated microwave field develops as

$$U_{\text{mic}}(z,t)=\chi_{\text{eff}}\delta\omega|U_0|^2$$

$$\times \text{Re}\left\{\frac{\exp\left[2i\,\delta\omega\left(t-\frac{z}{\nu_{\text{opt}}}\right)\right]\left[1-\exp\left(-\left\{\frac{\alpha_{\text{mic}}}{2}+2\alpha''_{\text{mic}}\delta\omega^2+2i\left[\delta\omega\left(\frac{1}{\nu_{\text{mic}}}-\frac{1}{\nu_{\text{opt}}}\right)+\frac{2}{3}\delta\omega^3 T_{\text{mic}}\right]\right\}z\right)\right]}{2\,\delta\omega\left(\frac{1}{\nu_{\text{mic}}}-\frac{1}{\nu_{\text{opt}}}\right)+\frac{4}{3}\delta\omega^3 T_{\text{mic}}-i\left[\frac{\alpha_{\text{mic}}}{2}+2\alpha''_{\text{mic}}\delta\omega^2\right]}\right\}. \tag{12a}$$

In the stationary state it oscillates at double the beat frequency, and the average power develops in the z direction as

$$\bar{p}_{\text{mic}}(Z)=\frac{1}{2}\frac{\chi_{\text{eff}}^2\delta\omega^2|U_0|^4}{\left[2\,\delta\omega\left(\frac{1}{\nu_{\text{mic}}}-\frac{1}{\nu_{\text{opt}}}\right)+\frac{4}{3}\delta\omega^3 T_{mic}\right]^2+\left[\frac{\alpha_{\text{mic}}}{2}+2\alpha''_{\text{mic}}\delta\omega^2\right]^2}$$

$$\times\left|1-\exp\left[-\left(\frac{\alpha_{\text{mic}}}{2}+2\alpha''_{\text{mic}}\delta\omega^2\right)z\right]\exp\left\{2i\left[\delta\omega\left(\frac{1}{\nu_{\text{mic}}}-\frac{1}{\nu_{\text{opt}}}\right)+\frac{2}{3}\delta\omega^3 T_{\text{mic}}\right]z\right\}\right|^2. \tag{12b}$$

Hence we find an oscillation of the microwave power, which in the presence of microwave losses are damped and a stationary state is approached (see Fig. 2). Hence the length of a microwave generator based on optical rectification should be chosen carefully to obtain optimum results. The maximum generated microwave power can be as much as four times as high as the value finally approached in the stationary limit.

B. Pulsed pump fields in non-velocity-matched geometries

The rather low conversion efficiency obtained for two interacting continuous waves considered above suggests that higher peak powers are required, and therefore a pulse beam excitation should be preferable. If no special care is taken to match the group velocities of the optical and microwave fields, the nondispersive terms are by far dominant in Eq. (10a). To simplify the analytical treatment, we therefore neglect all dispersive effects and take into account the nondispersive damping of the microwave only (i.e., $\alpha''_{\text{mic}}=T_{\text{mic}}=0$). To demonstrate that these assumptions are justified for non-velocity-matched configurations, we have also modeled the full system of equations (10) with the parameters of the structure depicted in Fig. 1 (see Fig. 3).

Assuming that the field propagation starts at $z=0$,[1] the resulting solution can be obtained by simple integration as

$$U_{\text{mic}}(z,t)=U_{\text{mic}}^0(t-z/\nu_{\text{opt}})-U_{\text{mic}}^0(t-z/\nu_{\text{mic}})\exp\left(-\frac{\alpha_{\text{mic}}}{2}z\right). \tag{13a}$$

The pulse shape, which enters Eq. (12), is given by

$$U_{\text{mic}}^0(t')=\frac{\chi_{\text{eff}}}{\frac{1}{\nu_{\text{mic}}}-\frac{1}{\nu_{\text{opt}}}}\left\{|U_{\text{opt}}(t')|^2-\frac{\alpha_{\text{mic}}/2}{\frac{1}{\nu_{\text{mic}}}-\frac{1}{\nu_{\text{opt}}}}\int_{\pm\infty}^{t'}dt''|U_{\text{opt}}(t'')|^2\exp\left[\frac{\alpha_{\text{mic}}/2}{\frac{1}{\nu_{\text{mic}}}-\frac{1}{\nu_{\text{opt}}}}(t''-t')\right]\right\}, \tag{13b}$$

---

[1]Strictly speaking, this boundary condition corresponds to a transmission line extending to $\pm\infty$ with zero nonlinearity for $z<0$. A terminated transmission line can be similarly analyzed with a boundary condition of zero current at $z=0$, but this solution only introduces a small, quasistatic term that can be neglected in most instances.
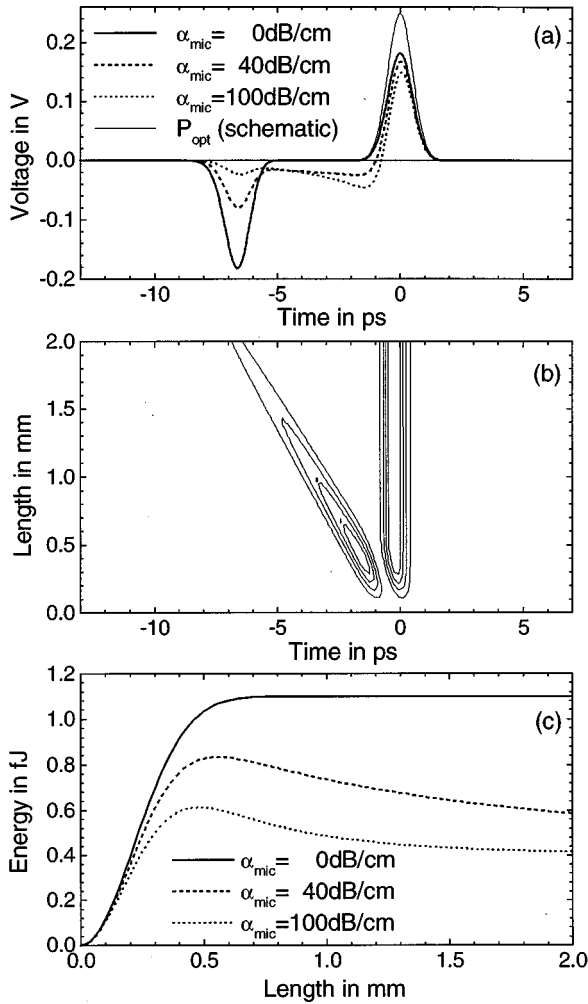
FIG. 3. Field propagation in a non-velocity-matched geometry simulated with the full set of equations (10) (all parameters as given in Table I; propagation length: 2 mm; reference frame: copropagating with the optical pulse). (a) Voltage pulse at the output for three different values of microwave losses. (b) Contour plot of the microwave power ($\alpha_{mic} = 40$ dB/cm; input position of the optical pulse: $t = 0$; contour lines: each 100 μW), and evolution of the total microwave energy for three different values of microwave losses.

where the positive (negative) signs refer to the cases where the velocity of the microwave is larger (smaller) than that of the optical field.

Obviously the excited microwave field consists of two parts [see Eq. (12a)], one traveling together with the optical pulse (velocity ν_{opt}), and another moving with the speed of the microwave ν_{mic} [see Fig. 3(a)]. Consequently the development of the system is characterized by two rather different scales. No further growth of the microwave field around the optical pulse occurs after the microwave pulses have separated from each other. The respective walk-off length is defined as

$$Z_{\text{walk-off}} \cong \frac{T_{\text{pulse}}}{\left| \dfrac{1}{\nu_{\text{mic}}} - \dfrac{1}{\nu_{\text{opt}}} \right|}, \qquad (14a)$$

and amounts to about 300 μm in our example (see Table I and Fig. 3). Since the evolution of the optical pulse occurs on

a much longer scale, the microwave pulse will follow the optical one while constantly adapting its shape according to Eq. (13b).

In contrast, a microwave signal which has left the optical pulse is subject to internal losses. Its absorption length (usually several millimeters or even centimeters) defines a second scale,

$$Z_{\text{abs}} \cong \frac{1}{\alpha_{\text{mic}}}, \qquad (14b)$$

after which we find stationary conditions and only the first pulse remains. In non-velocity-matched geometries the walk-off distance is usually much shorter than the absorption length. Within the approximations made here, there is no advantage in device lengths longer than this absorption length. In case of vanishing losses the electrical signal attached to the optical pulse is the exact image of the optical intensity distribution [see Fig. 3(c)]. With the nonlinear polarization acting as a source for the microwave, losses do not result in its extinction but only in a deformation of its shape.

This complicated dynamical behavior is reflected by the evolution of the electrical energy. It approaches a maximum value when both pulses have just separated. It then returns to about half this value if the second pulse is absorbed [see Fig. 3(b)]. The maximum possible conversion efficiency is obtained in the absence of absorption, i.e., if the energy of the second pulse is preserved. In case of a Gaussian-shaped input, $U_{\text{opt}}(t) = \sqrt{p_{\text{max}}} \exp(-t^2/T_{\text{pulse}}^2)$, and, neglecting absorption, the conversion efficiency defined as the relation of optical and microwave energies is given

$$\eta = \frac{Q_{\text{mic}}}{Q_{\text{opt}}} = \frac{2}{\sqrt{\pi}} \frac{\chi_{\text{eff}}^2}{\left(\dfrac{1}{\nu_{\text{mic}}} - \dfrac{1}{\nu_{\text{opt}}} \right)^2} \frac{Q_{\text{opt}}}{T_{\text{pulse}}}. \qquad (15)$$

For typical frequency conversion the efficiency is proportional to the optical power and the square of the nonlinear coefficient. Compared with second-harmonic generation the group-velocity mismatch plays a role similar to that of the phase mismatch. As already stated in Ref. [14], the group-velocity mismatch influences the conversion efficiency critically. In the case of an unmatched configuration in the present example (see Table I), an efficiency of 8.8×10^{-7} is obtained. In the case of a backward-propagating wave the velocity mismatch is considerably higher. Even in the case of a non-velocity-matched configuration, as studied above, the backward-propagating wave corresponds to only 2.7% of the total generated microwave power.

As already mentioned, the electrical pulse in its final state is an almost exact image of the optical signal. This remarkable property of non-velocity-matched configurations can be potentially employed as a basis for a photodetector with an extremely high temporal resolution. Another consequence of the low conversion efficiency is that the optical pulse is almost unaffected by the measurement. Hence an optical signal can be recorded in a quasitransparent geometry, and later it may be used for further applications.

Finally a comparison with second-harmonic generation shall be made. Although the evolution equations look very different, the basic scaling properties are the same due to the

TABLE I. Characteristics parameters of the structure depicted in Fig. 1. The wavelength selected here is for illustrative purposes only, and, although it lies with the two-photon absorption band of GaAs, this nonlinear loss process is neglected. In practice it would probably be necessary to employ a combination of alloy composition and wavelength corresponding to sub-half-band-gap frequencies.

Quantity		Symbol	Value
structure optical properties	group index	n_{opt}^{group}	3.55
	group-velocity dispersion	D_{opt}	1.3×10^{-24} s^2/m
structure microwave properties	impedance	Z	53.6 Ω
	group index	n_{mic}^{group}	2.55
	dispersion of the damping	α''_{mic}	0
	third-order dispersion	T_{mic}	1.1×10^{-35} s^3/m
structure electro-optic properties	nonlinear coefficient	χ_{eff}	-8.3×10^{-14} s/m$\sqrt{W}$
	electro-optic coefficient	$-\dfrac{2\omega_0 \chi_{eff}}{\sqrt{Z}}$	$28.4\dfrac{1}{mV}$
optical pulse (Gaussian)	wavelength	λ	1.5 μm
	duration	T_{pulse}	1 ps
	peak power	$p_{max} = |U_{opt}^{max}|^2$	1 kW
	pulse energy	Q_{opt}	1.25 nJ

quadratic interaction involved. However, a remarkable difference is the absence of an oscillatory behavior. While in non-phase-matched geometries up and down conversion of the second-harmonic power alternate, a stationary state is readily approached in case of non-velocity-matched optical rectification. The reason for this somehow unexpected behavior is that the rectification process produces a response centered at zero frequency, and therefore the phase of the optical wave does not influence the microwave field. Nevertheless interference between different microwave components can still play an important role. The formation of the steady state given by Eq. (13b) can be understood as a microwave field generated at one slope of the optical pulse, which then crosses the optical pulse due to the respective velocity difference, and is finally eliminated while interfering with microwave components generated at the other slope of the optical pulse.

C. Dispersive effects on the microwave propagation

Before dealing with the velocity-matched case, a short comment will be made with regard to the influence of the higher-order dispersive terms in Eq. (10a). By numerical simulations of non-velocity-matched configurations on the basis of the complete system of equations, it is found that the influence is almost negligible. In any case it is observed that the only significant effect is on the second pulse, which separated from the optical wave at the beginning. Provided that it is not already absorbed by strong losses, it starts to spread due to the influence of third-order dispersion. In contrast, the pulse attached to the optical signal remains almost unaffected. Only for very long propagation distances can a certain influence be perceived. However, if this is the case, the changes in the pump wave can no longer be ignored. Therefore, we come back to this point later in Sec. IV.

D. Velocity-matched structures

Now let as assume that our main focus is not a fast-response photodiode but an effective microwave generator, and that a considerable increase in the conversion efficiency is required. For the purpose it is essential to achieve velocity matching between the microwave and optical modes. Recently much effort has been devoted to achieving this goal. In traveling-wave geometries the efficiency of electro-optic modulation can be greatly enhanced if electrical signals and optical fields propagate with the same velocity. While the influence on the optical mode is basically limited, the speed of the microwave field can be easily modified. Almost complete velocity matching while maintaining low losses was reported in Ref. [15]. In the optimum case the group velocities of both waves coincide, the walk-off distance defined in Eq. (14a) diverges, and expression (13) is no longer valid. Then the microwave field evolves in the absence of dispersive effects as

$$U_{mic}(z,t) = 2 \frac{\chi_{eff}}{\alpha_{mic}} \left[1 - \exp\left(-\frac{\alpha_{mic}}{2} z \right) \right] \frac{\partial}{\partial t} |U_{opt}(t)|^2.$$

(16)

Note that the temporal field structure has changed from the non-velocity-matched case [see Fig. 4(a)], being proportional to the derivative of the optical power, rather than the optical power itself. The main reason for this is the significance the velocity mismatch term in Eq. (10a). In the limit of vanishing absorption, Eq. (16) indicates that the field grows linearly with z, and that the evolution of the pump wave can no longer be neglected above a certain rate of conversion. In the case of a Gaussian pulse (energy Q_{opt} and duration T_{pulse}) the conversion efficiency η in a velocity-matched structure amounts to

$$\eta(z) = \frac{Q_{\text{mic}}}{Q_{\text{opt}}} = \frac{8}{\sqrt{\pi}} \chi_{\text{eff}}^2 \left[\frac{1 - \exp(-\alpha_{\text{mic}} z/2)}{\alpha_{\text{mic}}} \right]^2 \frac{Q_{\text{opt}}}{T_{\text{pulse}}^3}.$$

$$(17)$$

In the case of vanishing losses, expression (17) grows proportionally to the square of the length. Note the much stronger dependence on the pulse duration compared with non-velocity-matched configurations [see Eq. (15)]. Hence optical rectification is much more efficient for ultrashort pulses. In the case of the structure depicted in Fig. 1 and for typical pulse parameters (Table I), a conversion efficiency of 1% is reached after a propagation length of 3.2 cm.

Coming back to the pulse shape described by Eq. (16), we find that for a typical optical pulse the spectrum of the generated microwave now exhibits a nonzero carrier frequency. To a certain extent one may regard the generated microwave as a single-cycle pulse with a carrier frequency defined by the pulse duration as

$$\omega_{\text{mic}} \approx \frac{2}{T_{\text{pulse}}}.$$

$$(18)$$

Because the rectification process is insensitive to the optical phase, one may easily tune this carrier frequency by changing the duration of the optical pulse by e.g. dispersive broadening.

A simulation based on the complete set of equations [see Fig. 4(a)] shows certain deviations from the analytical results obtained above. Due to the much longer propagation distance, the third-order dispersion of the microwave starts to play a considerable role and the emitted radiation is now obvious. Also the optical pulse is now depleted by the action of the nonlinearity, and can no longer regarded to be constant [see Fig. 4(c)].

IV. INFLUENCES ON THE PUMP WAVE

In a first instant one would guess that for the low conversion efficiencies reported above the pump wave remains unaffected. Numerical investigations reveal that although the power of the optical pulse does not significantly change there is a nonlinear evolution in its shape. The reason for this behavior is the action of the microwave on the optical field via the electro-optic effect. Already for a rather low conversion efficiency, as in the example depicted in Fig. 4, the induced voltage reaches a peak value of 6.1 V which is of comparable magnitude to those used in electro-optic modulators. Its influence on the propagation of the optical field is considerable because it induces a π phase shift after 1.8 cm of propagation.

In the case of a non-velocity-matched configuration (see Table I), we can estimate this action on the optical field by a pseudocubic nonlinearity which is characterized by an effective cubic coefficient γ_3 as

$$\gamma_3 = \frac{2\omega_{\text{opt}} \chi_{\text{eff}}^2}{\dfrac{1}{v_{\text{opt}}} - \dfrac{1}{v_{\text{mic}}}},$$

$$(19)$$

which amounts to about $\gamma_3 = -5.2 \times 10^{-3} \, \text{m}^{-1} \text{W}^{-1}$ in the case of our non-velocity-matched sample. This value is about
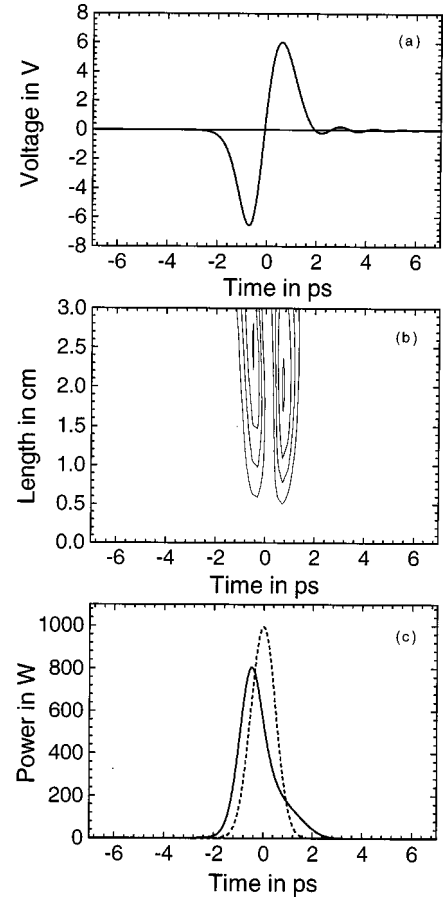
FIG. 4. Field evolution in a velocity-matched configuration (parameters as in Table I, except for the group indices $n_{\text{mic}}^{\text{group}} - n_{\text{opt}}^{\text{group}} = 0$ and propagation length: 3 cm, $\alpha_{\text{mic}} = 5$ dB/cm). (a) Voltage pulse at the output. (b) Contour plot of the microwave power (input position of the optical pulse: $t = 0$; contour lines: each 0.2 W). (c) Optical pulse at the input (dashed line) and at the output (solid line).

three orders of magnitude smaller than the comparable coefficient ($\propto n_2 / A_{\text{eff}}$) which originates from intrinsic cubic nonlinearities. However, there is considerable scope for enhancing this effect by improving the velocity matching in a slow wave structure, and, furthermore, by tuning the sign of the velocity difference the sign of the effective cubic nonlinearity can be changed. Hence a negative effective nonlinearity can be induced which would allow for soliton formation under the presence of normal group-velocity dispersion, as is usually found in semiconductors. In numerical simulations of a velocity-matched structure [see Fig. 4(b)], we indeed observed a considerable narrowing of the optical pulse instead of dispersive spreading. This effective third-order nonlinearity arising from a cascade of second-order nonlinearities has been extensively studied with reference to second-harmonic generation [16]. There are, however, a number of differences with the rectification cascade process; for example, the phase of the intermediate frequency is irrelevant here.

Of course in more detailed investigations the intrinsic third-order nonlinearity of the semiconductor has to be taken into account as well, and may balance the index changes induced by the rectification process to a certain extent. A detailed analysis of this nonlinear interaction is beyond the scope of this paper, and will be considered elsewhere.

V. CONCLUSIONS

We have derived a set of evolution equations which describes the mutual propagation of optical and microwave pulses linked together by a quadratic nonlinearity of the material. In the case of small conversion efficiencies, which is by far the most realistic, analytical expressions are derived which describe the generation of microwave signals. It turns out that in non-velocity-matched configurations a steady state is quickly approached, and no further evolution is observed beyond a certain propagation length. The generated microwave pulse is an almost exact image of the optical one, making optical rectification suitable for fast and distortion-free pulse detection. For velocity-matched configurations, much higher conversion efficiencies can be achieved. In this case the action of the generated electrical voltage on the optical pulse via the electro-optic effect has to be taken into account. It leads to an effective cubic nonlinearity which may allow for soliton formation.

[1] P. A. Franken, A. E. Hill, C. W. Peters, and G. Weinreich, Phys. Rev. Lett. **7**, 118 (1961).

[2] J. A. Armstrong, N. Blombergen, J. Duccing, and P. S. Pershan, Phys. Rev. **127**, 1918 (1962).

[3] M. Bass, P. A. Franken, J. F. Ward, and G. Weinreich, Phys. Rev. Lett. **9**, 446 (1962).

[4] Y. H. Jin and X.-C. Zhang, J. Nonlinear Opt. Phys. Mater. **4**, 459 (1995).

[5] A. Bonvalet, M. Joffre, J. L. Martin, and A. Migus, Appl. Phys. Lett. **67**, 2907 (1995).

[6] A. Nahata and T. F. Heinz, Opt. Lett. **23**, 867 (1998).

[7] D. Jäger, J. Phys. Soc. Jpn. **51**, 1686 (1982).

[8] D. Jäger, Int. J. Electron. **58**, 649 (1985).

[9] C.-K. C. Tzuang and J.-D. Tseng, IEEE Trans. Microwave Theory Tech. **39**, 1701 (1991).

[10] H. E. Green, IEEE Trans. Microwave Theory Tech. **13**, 676 (1965).

[11] A. P. Ansbro and I. Montrosset, IEE Proc.-J: Optoelectron. **140**, 254 (1993).

[12] T. Y. Chang, N. van Tran, C. K. N. Patel, Appl. Phys. Lett. **13**, 357 (1968).

[13] Y. R. Shen, *The Principles of Nonlinear Optics* (Wiley, New York, 1984).

[14] A. Bonvalet, M. Joffre, J. L. Martin, and A. Migus, Appl. Phys. Lett. **67**, 2907 (1995).

[15] R. G. Walker, IEEE J. Quantum Electron. **27**, 654 (1991).

[16] G. I. Stegeman, D. J. Hagan, and L. Torner, Opt. Quantum Electron. **28**, 1691 (1996).